Journal of Physical Sciences, Vol. 14, 2010, 31-44
ISSN: 0972-8791, www.vidyasagar.ac.in/journal
Published on December 24, 2010

Radiative Heat Transfer to MHD Couette Flow with Variable Wall Temperature and General Magnetic Boundary Conditions

N. Ghara, S. L. Maji, S. Das and R. N. Jana[1]

Department of Applied Mathematics with Oceanology and Computer Programming,
Vidyasagar University, Midnapore 721 102, INDIA
[1]jana261171@yahoo.co.in

Received October 15, 2010; accepted November 10, 2010

ABSTARCT

The problem of radiative heat transfer to magnetohydrodynamic Couette flow of a viscous incompressible electrically conducting fluid confined between infinite parallel conducting walls with variable walls temperature has been studied. An exact solution of the governing equations has been obtained in a closed form. It is found that the velocity at any point decreases while the temperature at any point increases with an increase in wall conductance. The induced magnetic field is strongly affected by the magnetic field as well as wall conductances. Further, the critical Eckert number for which there is no flow of heat either from walls to the fluid or fluid to the walls has been obtained. It is found that the critical Eckert number at the upper wall increases with an increase in either wall conductance parameter or radiation parameter.

Keywords: Couette flow, induced magnetic field, critical Eckert number.

1 Introduction

The problem of the MHD Couette flow of a viscous incompressible electrically conducting fluid with conducting walls has many practical applications in Astrophysics, Engineering and Space Science. Hydromagnetic Couette flow has been studied by Pai [1], Muhuri [2], Katagiri [3], Steinheuer [4] and Zierep and Buhler [5] and many others. Rao [6] considered the flow in a channel with conducting walls in the presence of a heat source/sink term as a model for Couette flow with variable wall temperature. Ogulu and Mosta [7] have studied the radiative heat transfer to magnetohydrodynamic Couette flow with variable wall temperature for conducting walls. They have solved the energy equation on using the Runge-Kutta and the Newton-Raphson shooting algorithm.

The aim of the present study is to investigate the combined effects of the radiative heat transfer and wall conductances on the MHD Couette flow with variable wall temperature. An exact analytical solution for the velocity field, the

induced magnetic field and the energy equation has been obtained in a closed form. So there is no need of the Runge-Kutta and the Newton-Raphson shooting algorithm for solving the energy equation as done by Ogulu and Mosta [7]. It is found that the velocity at any point decreases while the temperature at any point increases with an increase in wall conductance. The induced magnetic field is strongly affected by the magnetic field as well as wall conductances. Further, the critical Eckert number for which there is no flow of heat either from upper wall to the fluid or fluid to the upper wall has been obtained. It is found that the critical Eckert number at the upper wall increases with increase in either wall conductance parameter $\varphi \left(= \varphi_l + \varphi_u \right)$ or radiation parameter Ra .

2 Formulation of the problem and its solutions

Consider a steady MHD Couette flow of a viscous incompressible electrically conducting fluid confined between infinite conducting walls. The walls are at a distance $2L$ apart. Choose a cartesian coordinates system in such a way that the origin is at the middle of the channel, the x-axis is taken in direction of the flow, the y-axis perpendicular to it and z-axis is normal to the xy-plane. The upper wall moves with a uniform velocity U_0 in the direction of x-axis. A uniform magnetic field H_0 is applied perpendicular to the walls [See Fig.1].

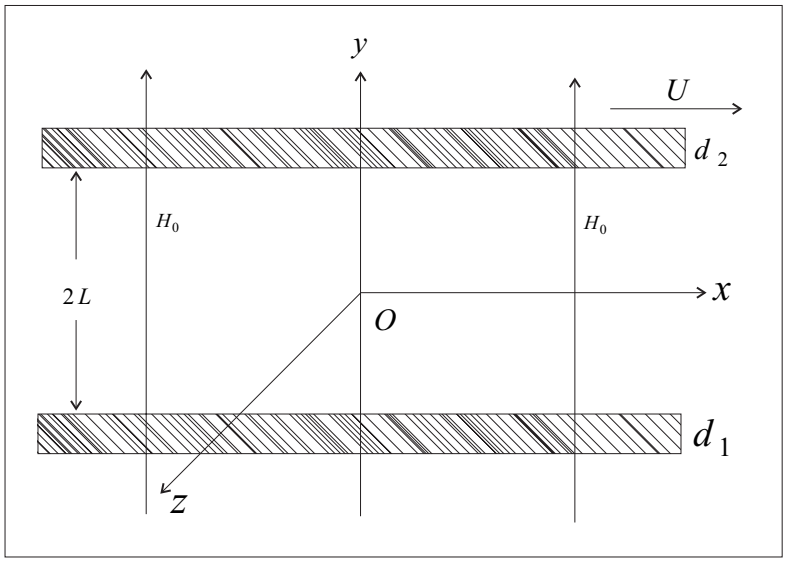

Fig.1: Geometry of the problem

Since the walls are infinitely long along x- and y- directions, all physical quantities will be functions of y only. The equation of continuity $\nabla \cdot \vec{q} = 0$ gives $\frac{du}{dx} = 0$ which implies that $u = u(y)$. Similarly the solenoidal relation $\nabla \cdot \vec{H} = 0$ yields $H_y = H_0$.

The momentum and magnetic induction equations which are comparatable with $\vec{q} = (u,0,0)$ and $\vec{H} = (H_x, H_0, 0)$ are respectively

$$\nu \frac{d^2u}{dy^2} + \frac{\mu_e H_0}{\rho} \frac{dH_x}{dy} = 0, \tag{1}$$

$$\frac{d^2H_x}{dy^2} + \sigma\mu_e H_0 \frac{du}{dy} = 0, \tag{2}$$

where ν is the kinematic coefficient of viscosity and ρ is the density of the fluid, σ the electrical conductivity of the fluid and μ_e the magnetic permeability.

The velocity boundary conditions are the no-slip conditions at the walls

$$u = 0 \text{ at } y = -L \text{ and } u = U_0 \text{ at } y = L. \tag{3}$$

The magnetic boundary conditions at the walls $y = -L$ and $y = L$ can be derived as follows. From equations $\nabla \times \vec{H} = \vec{j}$ and $\vec{j} = \sigma\left(\vec{E} + \mu_e \vec{q} \times \vec{H}\right)$, we have

$$\frac{dH_x}{dy} = -\sigma\left(E_z + \mu_e H_0 v_x\right), \tag{4}$$

$$j_x = \sigma E_x, \tag{5}$$

the equation $\nabla \times E = 0$ gives $E_x = E_z$=constant within the solid boundaries as well as within the fluid and σ is the electrical conductivity of the fluid .

Within the lower wall $(y = -L)$, we get

$$\frac{dH_x^{(s)}}{dy} = -\sigma_1 E_z, \tag{6}$$

where σ_1 is the electrical conductivity of the lower wall and the superscripts (s) denotes the quantities within the solid. Integrating equation (6), we have

$$H_x^{(s)} = -\sigma_1 E_z y + c_1. \tag{7}$$

At the outer surface $y = -(L + d_1)$ the following condition is satisfied

$$H_x^{(s)}\left(-L - d_1\right) = 0,$$

which in turn gives

$$c_1 = -\sigma_1 E_z (d_1 + L). \tag{8}$$

Hence

$$H_x^{(s)} = -\sigma_1 E_z \left(y + L + d_1\right). \tag{9}$$

At the lower wall $y = -L$ (the interface between the wall and the fluid)

$$H_x^{(s)}(-L) = -\sigma_1 E_z d_1, \tag{10}$$

Within the fluid $y = -L$, we have

$$\frac{dH_x}{dy} + \sigma E_z = 0. \tag{11}$$

For the continuity of the tangential component of E_z, we have from equations (10) and (11)

$$\frac{dH_x}{dy} - \frac{\sigma H_x}{\sigma_1 d_1} = 0 \text{ at } y = -L. \tag{12}$$

Within the upper wall $(y = L)$, we have

$$\frac{dH_x^{(s)}}{dy} = -\sigma_2 E_z, \tag{13}$$

where σ_2 is the electrical conductivity of the upper wall.

Integrating (13) and using the conditions $H_x^{(s)}(L + d_2) = 0$, we find, at $z = L$, the interface between the fluid and the wall

$$H_x^{(s)}(d) = \sigma_2 E_z d_2. \tag{14}$$

At the upper wall $(y = L)$, equation (4) gives

$$\frac{dH_x}{dy} = -\sigma(E_z + \mu_e H_0 U_0). \tag{15}$$

For the continuity of tangential components of the electric field, we have from equations (14) and (15) as

$$\frac{dH_x}{dy} + \frac{\sigma H_x}{\sigma_2 d_2} = -\sigma \mu_e H_0 U_0 \text{ at } y = L. \tag{16}$$

Introducing the non-dimensional variables

$$\eta = \frac{y}{L}, u_1 = \frac{u}{U_0} \text{ and } h_x = \frac{H_x}{\sigma \mu_e \nu H_0}, \tag{17}$$

equations (1) and (2) become

$$\frac{d^2 u_1}{d\eta^2} + \frac{M^2}{\text{Re}} \frac{dh_x}{d\eta} = 0, \tag{18}$$

$$\frac{d^2 h_x}{d\eta^2} + \text{Re} \frac{du_1}{d\eta} = 0, \tag{19}$$

where $M^2 = \mu_e H_0^2 \left(\frac{\sigma}{\rho \nu} \right)^{1/2}$ is the Hartmann number and $\text{Re} = \frac{U_0 L}{\nu}$ the Reynolds number.

The corresponding boundary conditions for u_1 and h_x are

$$u_1 = 0 \text{ at } \eta = -1 \text{ and } u_1 = 1 \text{ at } \eta = 1, \tag{20}$$

$$\frac{dh_x}{d\eta} - \frac{h_x}{\varphi_l} = 0 \text{ at } \eta = -1 \text{ and } \frac{dh_x}{d\eta} + \frac{h_x}{\varphi_u} = -\text{Re} \text{ at } \eta = 1. \tag{21}$$

where $\varphi_l = \frac{\sigma_1 d_1}{\sigma L}$ and $\varphi_u = \frac{\sigma_2 d_2}{\sigma L}$ are the dimensionless wall conductance ratios.

The solution of the equations (18) and (19) subject to the boundary conditions (20) and (21) are

$$u_1(\eta) = a\left(1 - \frac{\cosh M\eta}{\cosh M}\right) + \frac{\sinh M(1+\eta)}{\sinh 2M}, \tag{22}$$

$$h_x(\eta) = R_e\left[\frac{a\sinh M\eta}{M\cosh M} - \frac{\cosh M(1+\eta)}{M\sinh 2M}\right] + \frac{\mathrm{Re}}{2}\left[\frac{1+\cosh 2M}{M\sinh 2M} - a(\varphi_u - \varphi_l)\right], \tag{23}$$

where

$$a = \frac{1}{(\varphi_l + \varphi_u)M\coth M + 2}. \tag{24}$$

It is seen from the expressions (22)-(24) that the velocity depends only on the sum of the wall conductances φ_l and φ_u but the induced magnetic field depends on the sum of the wall conductances φ_l and φ_u as well as the individual values of φ_l and φ_u.

The results of this paper can not be compared with the result of Ogulu and Mosta [7] because the boundary conditions of the induced magnetic field prescribed by Ogulu and Mosta [7] are incorrect. The correct boundary conditions, according to Ogulu and Morta [7], of the induced magnetic field will be

$$\frac{dh_x}{d\eta} - \frac{h_x}{\varphi_l} = 0 \text{ at } \eta = -1 \text{ and } \frac{dh_x}{d\eta} + \frac{h_x}{\varphi_u} = -\mathrm{Re} \text{ at } \eta = 1. \tag{25}$$

The solution of equations (18) and (19) subject to boundary conditions (20) and (46) (Ogulu and Mosta [7]) are

$$u_1(\eta) = -\frac{\sinh M\eta}{\sinh M}, \tag{26}$$

$$h_x(\eta) = \frac{\mathrm{Re}}{M^2}\left[\frac{\cosh M\eta}{\sinh M} + \coth M\right]. \tag{27}$$

It is observed from the equations (26) and (27) (Ogulu and Mosta [7]) that the velocity field and induced magnetic field are independent of the wall conductances, φ_l and φ_u. This is due to the fact that walls are moving with the same velocity but in opposite directions.

3 Results and Discussion

To study the effects of the magnetic field and wall conductances on the MHD Couette flow, the dimensionless velocity and the induced magnetic field are depicted graphically against η in Figs.2-3 for several values of Hartmann number M and wall conductance $\varphi(=\varphi_l + \varphi_u)$. Fig.2 depicts the effect of the magnetic field and wall conductance on the velocity field. We notice from Fig.2 that for fixed value of φ, the velocity u_1 increases near the lower wall of channel, while near the upper wall it decreases with an increase in Hartmann number M. It is also noticed that at

any point the velocity u_1 decreases with increase in φ for fixed value of M. It is seen from Fig.3 that for fixed value of φ, the induced magnetic field h_x decreases in the range $-1 \le \eta \le 0.7$ while it increases in the range $0.7 < \eta \le 1.0$ with an increase in Hartmann number M. It is manifested that there is a closeness of the curves near the upper wall. Fig.3 reveals that for fixed value of M, the induced magnetic field h_x increases in magnitude in the range $-1 \le \eta \le 0.45$ and decreases in the range $0.45 < \eta \le 1.0$ with increase in φ.

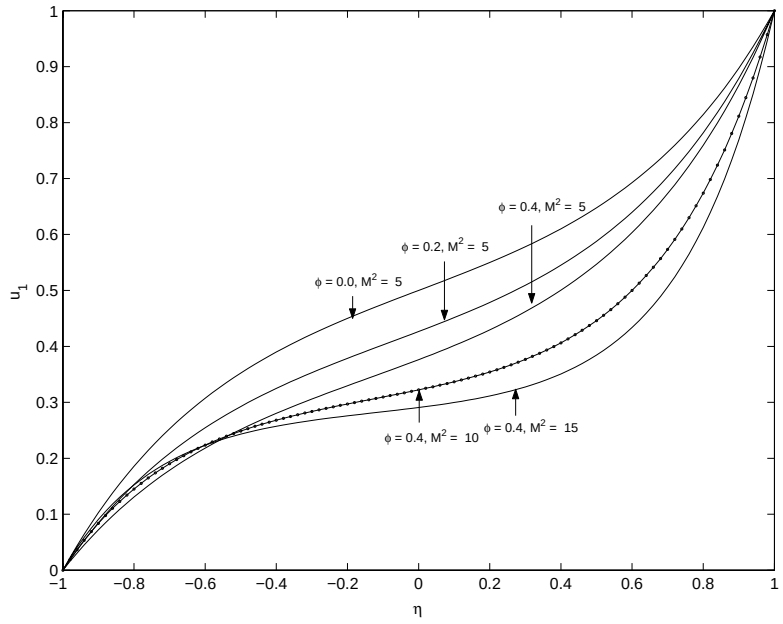

Fig.2: Variation of u_1 for $r_T = 0.2$.

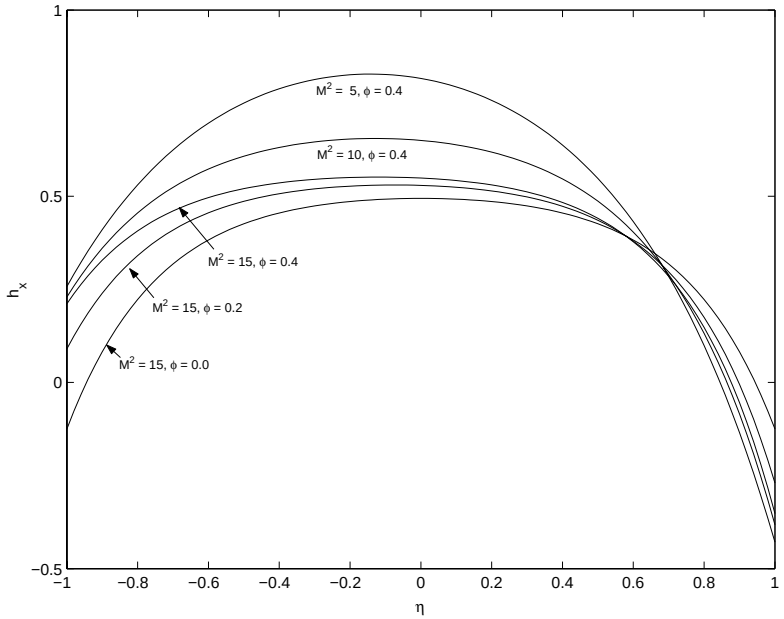

Fig.3: Variation of h_x for $r_T = 0.2$.

The non-dimensional shear stresses at the lower wall $\eta = -1$ and the upper wall $\eta = 1$ are respectively given by $\tau_l = \left(\frac{du}{d\eta}\right)_{\eta=-1}$ and $\tau_u = \left(\frac{du}{d\eta}\right)_{\eta=1}$ where

$$\left(\frac{du}{d\eta}\right)_{\eta=-1} = \frac{M\coth M}{(\varphi_l + \varphi_u)M\coth M + 2} + \frac{M}{\sinh 2M}, \tag{28}$$

and

$$\left(\frac{du}{d\eta}\right)_{\eta=1} = -\frac{M\coth M}{(\varphi_l + \varphi_u)M\coth M + 2} + M\coth 2M. \tag{29}$$

Numerical values of the non-dimensional shear stresses at the lower wall $\eta = -1$ and the upper wall $\eta = 1$ are shown graphically against M^2 for different values of φ in Fig.4. It is seen that the shear stress τ_l decreases while τ_u increases with an increase in φ when M is fixed. It is also seen that for fixed values of φ, τ_l increases steadily with increase in M^2. On the other hand, τ_u first decreases, reach a maximum and then increases with an increase in M^2.

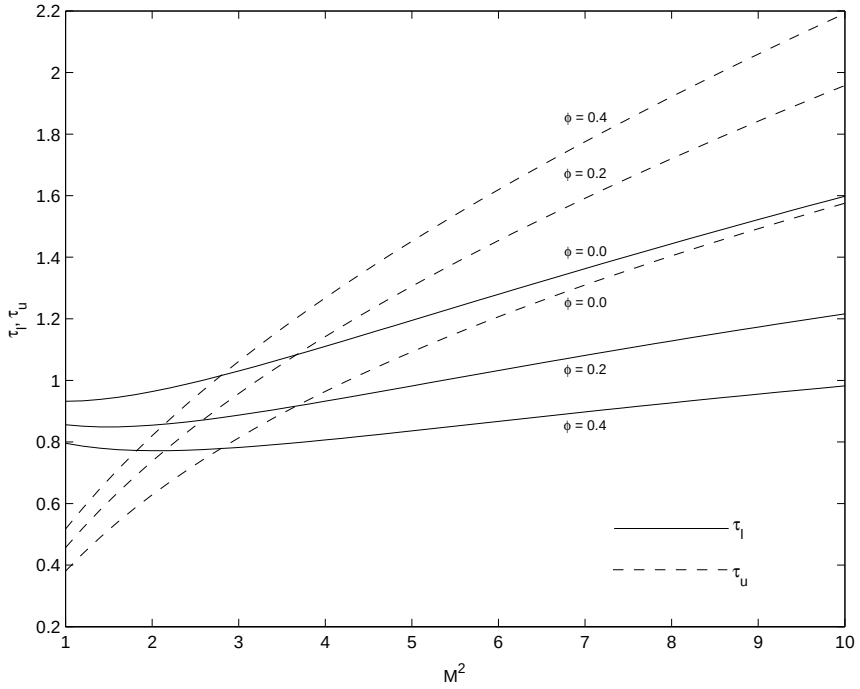

Fig.4: Variation of τ_l and τ_u for $r_T = 0.2$.

4 Heat Transfer

The equation of energy for the temperature distribution is

$$\rho c_p\, u \frac{\partial u}{\partial x} = k\left(\frac{\partial^2 T'}{\partial x^2} + \frac{\partial^2 T'}{\partial y^2}\right) + \mu\left(\frac{\partial u}{\partial y}\right)^2 + \frac{1}{\sigma}\left(\frac{\partial H_x}{\partial y}\right)^2 - \frac{\partial q'}{\partial y}, \tag{30}$$

where T', q', k, μ and c_p are respectively the temperature, the radiative flux, the thermal conductivity, kinematic coefficient of viscosity, specific heat of the fluid .
The Rossland approximation is assumed to hold and we have

$$q' = -\frac{4\sigma^*}{3k^*}\frac{\partial T'}{\partial y}, \tag{31}$$

where σ^* is the Stefan-Boltzman constant and k^* the mean absorption coefficient. We assumed that the temperature differences within the flow are sufficiently small such that T'^4 can be expressed as a linear function of temperature. We therefore expand T'^4 in a Taylor series about the temperature T_0 (T_0 being the temperature at $\eta = 0$), neglecting higher order terms to obtain

$$T'^4 \approx 4T_0^3 T' - 3T_0^4. \tag{32}$$

On using equations (31) and (32), equation (30) becomes

$$\rho c_p u \frac{\partial T'}{\partial y} = k\left(\frac{\partial^2 T'}{\partial x^2} + \frac{\partial^2 T'}{\partial y^2}\right) + \mu\left(\frac{\partial u}{\partial y}\right)^2 + \frac{1}{\sigma}\left(\frac{\partial H_x}{\partial y}\right)^2 + \frac{16\sigma^* T_0^3}{3k^*}\frac{\partial^2 T'}{\partial y^2}. \quad (33)$$

The boundary conditions for temperature distribution are

$$T' = T_1 \text{ at } y = -L \text{ and } T' = T_2 \text{ at } y = L, \quad (34)$$

where T_1, T_2 denote the temperatures of the lower and upper walls respectively.

We assume that the temperature varies linearly along the wall in addition to radiative heat transfer, so that

$$T'(x, y) = T(y) + N x. \quad (35)$$

On account of equation(35), equation (33) reduced to

$$\rho c_p \, Nu = \left(k + \frac{16\sigma^* T_0^3}{3k^*}\right)\frac{\partial^2 T}{\partial y^2} + \mu\left(\frac{\partial u}{\partial y}\right)^2 + \frac{1}{\sigma}\left(\frac{\partial H_x}{\partial y}\right)^2 \quad (36)$$

with the boundary conditions

$$T'(x, -L) = T(-L) + N x = T_1,$$
$$T'(x, L) = T(L) + N x = T_2. \quad (37)$$

Introducing

$$\theta = \frac{T - T_1}{T_2 - T_0}, \quad (38)$$

and using (17), equation (36) becomes

$$(1 + Ra)\frac{d^2\theta}{d\eta^2} = \lambda \,\mathrm{Re}\,\mathrm{Pr}\, u_1 - \mathrm{Pr}\, Ec\left[\left(\frac{du_1}{d\eta}\right)^2 + \frac{M^2}{\mathrm{Re}^2}\left(\frac{dh_x}{d\eta}\right)^2\right] \quad (39)$$

where $\mathrm{Pr} = \frac{\rho c_p \nu}{k}$ is the Prandtl number, $\lambda = \frac{NL}{T_2 - T_0}$ the temperature parameter, $Ec = \frac{U_0^2}{c_p (T_2 - T_0)}$ the Eckert number, $Ra = \frac{16\sigma^* T_0^3}{3k^* k}$ the radiation parameter and $r_T = \frac{T_2 - T_1}{T_2 - T_0}$ the temperature ratio.

The temperature boundary conditions (34) become

$$\theta = 0 \text{ at } \eta = -1 \text{ and } \theta = r_T \text{ at } \eta = 1, \quad (40)$$

The solution of the equation (39) subject to the boundary conditions (40) is

$$\theta(\eta) = \frac{\lambda \,\mathrm{Pr}\,\mathrm{Re}}{1 + Ra}\left[a\left(\frac{1}{2}\eta^2 - \frac{\cosh M\eta}{M^2 \cosh M}\right) + \frac{\sinh M(1 + \eta)}{M^2 \sinh 2M}\right]$$
$$- \frac{\lambda \,\mathrm{Pr}\,\mathrm{Re}}{1 + Ra}\left[\frac{a^2 \cosh 2M\eta}{4\cosh^2 M} + \frac{\cosh 2M(1 + \eta)}{4\sinh^2 2M} - \frac{a \sinh M(1 + 2\eta)}{2\cosh M \sinh 2M}\right]$$

$$+c_1\eta + c_2, \tag{41}$$

where

$$c_1 = \frac{1}{2}\left[r_T - \frac{\lambda \,\mathrm{Pr}\,\mathrm{Re}}{M^2\left(1+Ra\right)} - \frac{\mathrm{Pr}\,Ec}{1+Ra}\left(a-\frac{1}{2}\right)\right],$$

$$c_2 = \frac{1}{2}\left[r_T - \frac{\lambda \,\mathrm{Pr}\,\mathrm{Re}}{1+Ra}\left\{a\left(\frac{1}{2}-\frac{1}{M^2}\right)\right\} + \frac{\mathrm{Pr}\,Ec}{1+Ra}\left\{\frac{a^2\cosh 2M}{2\cosh^2 M} + \frac{1+\cosh 4M}{4\sinh^2 2M} + \frac{a\left(\sinh M - \sinh 3M\right)}{2\cosh M \sinh 2M}\right\}\right], \tag{42}$$

and a is given by (24). It is observed from the equations (41) and (42) that the temperature field depends only on the sum of the wall conductances φ_l and φ_u.

To study the effect of the radiation and the wall conductance on the temperature field θ, we have presented Fig.5 against η for various values of Ra and $\varphi\ (=\varphi_l+\varphi_u)$ with $M^2=5$ and $r_T=0.2$. Fig.4 shows that the temperature at any point increases with an increase in either φ or radiation parameter Ra.

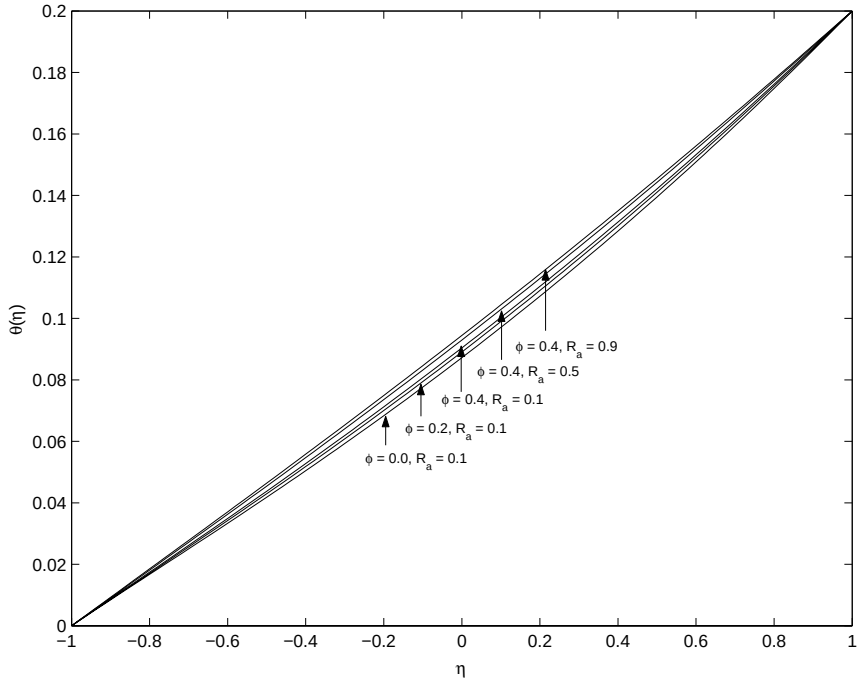

Fig.5: Variation of θ for $M^2=5, r_T=0.2$.

The rate of heat transfer at the walls $\eta=-1$ and $\eta=1$ are respectively given by

$$\left(\frac{d\theta}{d\eta}\right)_{\eta=-1} = \frac{1}{2}r_T - \frac{\lambda\,\mathrm{Pr}\,\mathrm{Re}}{1+Ra}\left[\frac{1}{2M^2} + a\left(1-\frac{\tanh M}{M}\right) + \frac{1}{M\sinh 2M}\right]$$

$$+\frac{\Pr \mathrm{Re}\, Ec}{1+Ra}\left[a^2 M \tanh M+\frac{a\,M}{\sinh 2M}+\frac{1}{2}\left(\frac{1}{2}-a\right)\right], \tag{43}$$

$$\left.\frac{d\theta}{d\eta}\right)_{\eta=1}=\frac{1}{2}r_T+\frac{\lambda \Pr \mathrm{Re}}{1+Ra}\left[a\left(1-\frac{\tanh M}{M}\right)+\frac{\coth 2M}{M}-\frac{1}{2M^2}\right]$$

$$-\frac{\Pr \mathrm{Re}\, Ec}{1+Ra}\left[\begin{array}{l}a^2 M \tanh M+M\coth 2M\\ -\dfrac{a\,M\cosh 3M}{\cosh M\sinh 2M}+\dfrac{1}{2}\left(a-\dfrac{1}{2}\right)\end{array}\right]. \tag{44}$$

The values of $\left.\frac{d\theta}{d\eta}\right)_{\eta=-1}$ and $\left.\frac{d\theta}{d\eta}\right)_{\eta=1}$ against M^2 are entered in Figs.6 and 7 for different values of Ra and φ with $\lambda=0.5$, $\Pr=0.025$ and $\mathrm{Re}=5$. It is seen from Fig.6 that the rate of heat transfer at the wall $\eta=-1$ increases with an increase in either φ or M^2. On the other hand, the rate of heat transfer at the wall $\eta=-1$ increases for $M^2\le 3.358$ and decreases for $M^2>0.358$ with an increase in Ra. Fig.7 shows that the rate of heat transfer at the wall $\eta=1$ decreases with an increase in either φ or Ra while it increases with an increase in M^2.

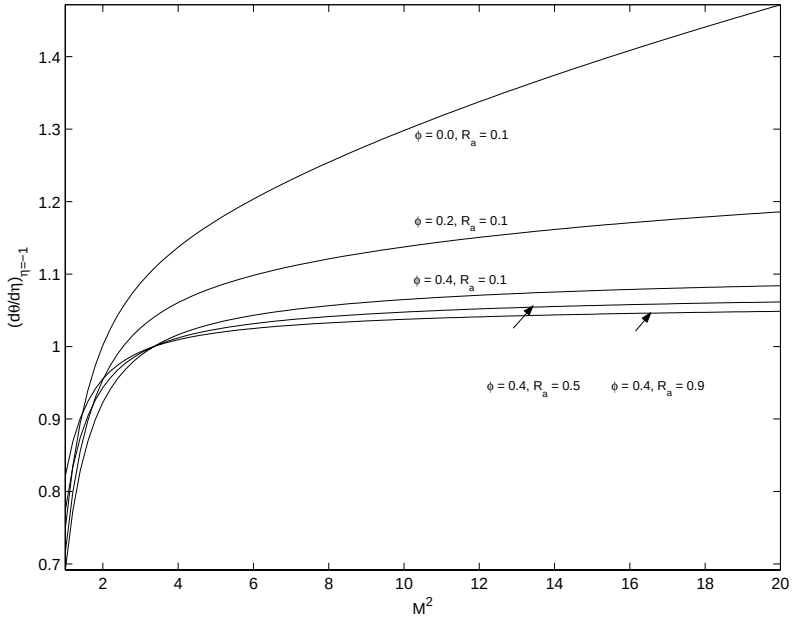

Fig.6: Variation of $\left(\frac{d\theta}{d\eta}\right)_{\eta=-1}$ for $r_T=0.2$.

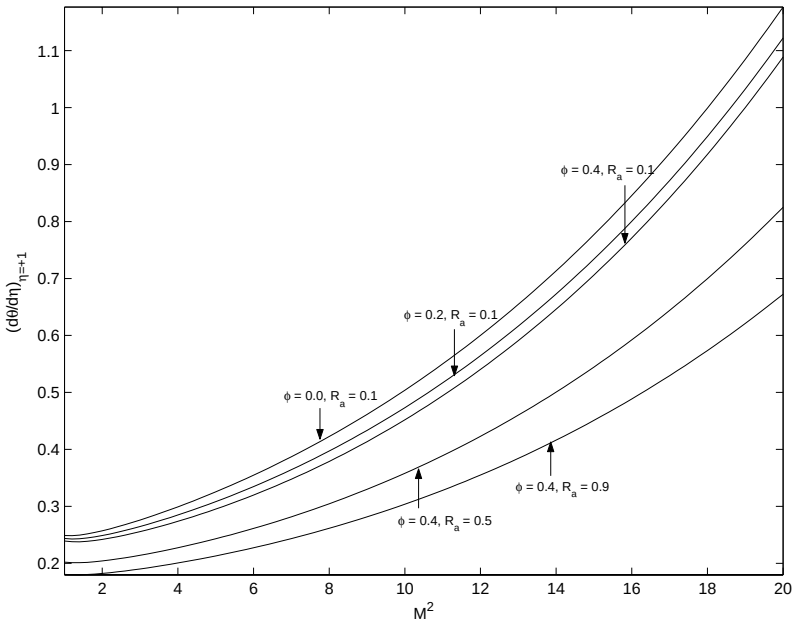

Fig.7: Variation of $\left(\frac{d\theta}{d\eta}\right)_{\eta=+1}$ for $r_T = 0.2$.

Equation (44) shows that, if $E_c = (E_c)_u$, where

$$(Ec)_u = \frac{\lambda \,\mathrm{Pr}\,\mathrm{Re}\left[a\left(1-\frac{\tanh M}{M}\right)+\frac{\coth M}{M}-\frac{1}{2M^2}\right]+\frac{1}{2}r_T\left(1+Ra\right)}{\mathrm{Pr}\left[a^2 M\tanh M + M\coth 2M - \frac{aM\cosh 3M}{\cosh M\sinh 3M}+\frac{1}{2}\left(a-\frac{1}{2}\right)\right]}, \tag{45}$$

then there is no flow of heat either from fluid to the upper wall or that from wall to fluid. Since $T_2 > T_0$, it follows from (44) that heat will flow from wall to the fluid if $Ec < (Ec)_u$, while heat will start flowing from fluid to the upper wall if $Ec > (Ec)_u$ even though the wall temperature is greater than the fluid temperature.

The value of $(Ec)_u$ computed for different values of φ and Ra is shown in Fig.8 against M^2. It is observed from Fig.8 that the critical Eckart number at the upper wall $(Ec)_u$ increases with increase in either φ or Ra. On the other hand $(Ec)_u$ decreases with an increase in squared-Hartmann number M^2.

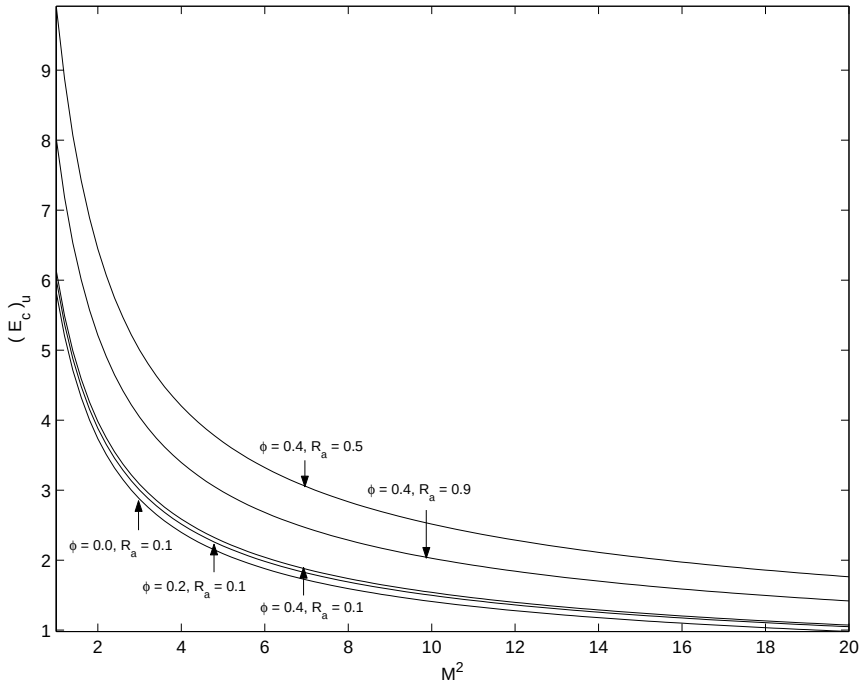

Fig.8: Variation of $(E_c)_u$ for $r_T = 0.2$.

Conclusion: The steady MHD Couette flow of a viscous incompressible electrically conducting fluid between infinite parallel conducting walls and radiative heat transfer has been studied in the presence of a uniform transverse applied magnetic field. Numerical results are presented to account the effect of the magnetic field and wall conductance on the flow field. The study reveals that the velocity field, induced magnetic field and temperature field are significantly affected by the wall conductance and the radiative heat.

The results of this paper can not be compared with the result of Ogulu and Mosta [7] because the boundary conditions of the induced magnetic field prescribed by Ogulu and Mosta [7] are incorrect.

REFERENCES

1. Pai, S.I.: Magnetogasdynamics and Plasma Dynamics, Viena, Springer-Verlag, New York, 1962
2. Muhuri, P.K.: Flow formation in Couette motion in magnetohydrodynamics with suction, J. Phys. Soc. Japan, vol.18, No.11,(1963), pp. 1671-1675.
3. Katagiri, M. : Flow formation in Couette motion in magnetohydrodynamics, J.Phys. Soc. Japan, vol.17, No.2, (1962), pp. 393-396.
4. Steinheuer, J.: Eine exakte Losung der instatinonaren Couette-Stromung,

Abhandlg. der Braunschweigischen wiss. Ges., vol.17, (1965), pp. 154-164.
5. Zierep, J. and Buhler, K.: Beschleunigte/ verzogerte platte mit homogenem Ausblasen/ Absaugen, Z. Angew. Math. Mech., vol. 73, (1993), pp.T527-T529.
6. Rao, S.V., Phys.Lett., 69A, 332 (1979).
7. Ogulu, O. and Motsa, S.: Radiative Heat Transfer to MHD Couette flow with variable Wall Temperature, Physica Scripta., vol.71, 336-339, 2005.